Bol. Soc. Paran. Mat.
©SPM – E-ISSN-2175-1188
SPM: www.spm.uem.br/bspm

(3s.) **v. 2026 (44) 4** : 1–21.
ISSN-0037-8712
doi:10.5269/bspm.80078

Pressure Gradient-Influenced Two Dimensional Unsteady Boundary Layer Viscous Flow Over a Flat Plate

Shilpa P., Nagaraj C., Rakesh Kumar Singh, Lakshmi B., Vatsala G. A.

ABSTRACT: We study unsteady behavior in 2D BL flow over a flat plate which is moving opposite to unsteady free-stream velocity. The system is described by the third-order nonlinear ordinary differential equation. Two approaches are used: the available exact solution for a particular set of parameters (k, β, λ) is modified, rewritten and used to obtain the solution in the convergent series form for other set of parameters and asymptotic behavior far away from the surface and for strong unsteadiness. There is a good agreement in predicting the wall shear stress and velocity profiles in the BL. The velocity profiles for the pressure gradient have the BL character analogous to the steady solutions. The findings indicate that when there is an adverse pressure gradient, both overshoots and undershoots occur close to the wall surface and move forward farther from the wall. The results are explored in detail.

Keywords: Unsteady boundary layers, pressure gradient, overshoot, undershoot.

Contents

1. Introduction

Unsteady BL flows are usually start-up motion from the rest or transition from one steady to another, and have significant practical applications such as in missile aerodynamics, in flutter phenomena that involves wings, in turbo machines, in aircraft reactions to atmospheric variations, propulsion of fish, etc. During last few years, this has been also a topic of interest in the fields of biomedical engineering (flow through the arteries, etc) and applied mathematics. Despite, this theory has be poorly developed compared to steady BL flow, mainly because the presence of an extra independent variable in the problem that increases the mathematical complexity. This unsteady in the model considerably changes the behavior of the flow including transient or non-parallel flow effects.

One other important applications where an unsteady BL forms around the flapping wings of the insects. When insect does the clap-fling-sweep manoeuvre. An unsteady BL forms close to the wing surface, and the Re of the wing motion is relatively big. It is assumed that these wings have flat sides. These wings are assumed to be side flat surfaces. If (r, θ) are the polar coordinates, then at a time t, both wings are at the position $\theta = +\alpha(t)$ and $\theta = -\alpha(t)$ because they rotate in opposite direction, and $\theta = 0$ is the axis of symmetry. The mainstream velocity $U(r, t)$ away from the wings's surface may be approximated by $U(r, t) \propto A(t)r^m$, where m is a constant and $A(t)$ is an arbitrary function that depends on time. (Kolomenskiy and Moffatt [1]) have obtained the similar derivation from the Lighthill's complex potential theory (Kolomenskiy *et* al. [2]) for the stagnation point flows ($m = 1$). This form closely relates to the above mainstream $U(r, t)$. This has motivated (partly) to study the unsteady effects on the flow with regard to the free parameter m which lead to new family of solutions. The effects of unsteadiness on

2020 *Mathematics Subject Classification:* 05C50,05C90.
Submitted November 11, 2025. Published February 26, 2026

BL flows is investigated which entirely depends on time variation of the mainstream flow. Our analysis also accommodates the velocity variation pertaining to the free-constant m on the BL. We will always link m to the pressure gradient in the boundary layer on the assumption of the mainstream flows. We will derive it in the next section.

In the BL, the pressure gradient along the direction normal is constant, the distribution of pressure depends only on x and time t. The free-stream flow is an unsteady, the pressure gradient can be obtained from the Prandtl's unsteady boundary layer equations (will be derived later), and also without having the details of the fluid flow in the boundary layer (Batchelor [3], Schlichting [4], Yuan [19]). For an unsteady laminar two-dimensional system in Cartesian coordinates, the mainstream flow is variation is taken in the form of the power-law relation which is proportional to $A(t)x^m$ where x is measured along the wedge surface and m is a constant. For steady flow and for $m = 0$, the case is the Blasius flow, and when $m = 1$, the case is stagnation point flow analyzed by the Hiemenz [5]. By assuming the above approximation, we are led to consider a class of flows of the Falkner-Skan are led to consider a class of flows of the Falkner- Skan type in the unsteady boundary-layer. Permitting the freestream velocity of the above form within boundary-layer, Dhanak and Duck [6] and Duck *et* al. [7] have shown that the three-dimensional boundary-layer flows lead to the Falkner-Skan type flows that encompass a more broad spectrum of important flow phenomena. For an inviscid flow, the Prandtl's boundary- layer equations can be matched to the mainstream (with the kinematic viscosity tends to zero) at which the pressure gradient equates to the mainstream flow. Therefore, the above constant m now corresponds to the pressure gradient variations. Far away from the wedge surface (inviscid flow), the Prandtl's boundary layer equations can be matched to the mainstream (with the kinematic viscosity tends to zero) at which the pressure gradient equates to the mainstream flow. Therefore, the above constant m now defines the strength of the pressure gradient. The arbitrary values of m introduces an additional parameter in the governing equation which increases complexity of the problem. When $m < 0$, the flow has an adverse pressure gradient ($\frac{\partial p}{\partial x} > 0$) and when $m > 0$, the flow becomes a favorable pressure gradient ($\frac{\partial p}{\partial x} < 0$). For steady flow, the theory is well established for the variable pressure gradient, however, the case is no longer true for an unsteady flow except for $m = 1$. Thus, the purpose of the present paper is partly to analyze the dependency of the pressure gradient on the unsteady laminar BL flow in detail, and in particular for an adverse gradient ($m < 0$) the solutions are of interest because the nature of the flow in the boundary layer could lead to boundary layer separation. This is discussed in detail (Kudenatti *et* al. [8]; Kudenatti *et* al. [9]; Hastings and Troy [10]. Furthermore, the moving wedge also plays an important role in the unsteady boundary layer flow, with a variable pressure gradient. As a result for various values of wedge speed, the thickness of the BL increases monotonically with it thereby the entire flow structure shall be discussed with regard to the wedge speed.

In a series of papers on the classical Falkner-Skan equation which is obtained from the steady two-dimension BL equations with the mainstream flows proportional to x^m, it has been shown that the problem admits a class of self-similar BL flows. In addition to this, the UBL equations also admit similarity-type solutions when the mainstream flow is of the same form. It is of course well known that the steady Falkner-Skan equation (Yang and Chien [11]; Riley and Weidman [12]; Sachdev *et* al. [13]; Kudenatti *et* al. [28] and the references therein) exhibits interesting BL solutions for various values of m, and some of the solutions are oscillatory in nature((Hastings and Troy [10]; Oskam and Veldman [14]; Kudenatti *et* al. [8]. On the other hand, the unsteady Falkner-Skan solutions are relatively benign in nature, and also exhibit oscillatory nature (Kudenatti *et* al. [25]). However, we are less interested in the global nature of the BL, rather we focus more on obtaining the solutions of the problem involving unsteady and pressure gradient and that admit aforementioned class.

Thus, we will study the effects of the pressure gradient and wedge speed on a general unsteady BL flow possessing the BL character. We shall develop a technique for unsteady BL problem that is more analytical in nature and hence this work is also applicable to the steady BL flows. Although this work is taken from (Sachdev *et* al. [13], the technique involves contribution of unsteady thereby making it fully rational. In fact these solutions describing unsteady flows are regarded as exact solutions of the Navier-Stokes equations in the BL limit. In a similar nature of work with suitable initial guess obtained by relaxing nonlinear terms, Liao [15] gave a homotopy analysis method for the problem involving BL flows in-terms of uniformly valid solution. Numerical computation of unsteady two-dimensional BL flow

is reported in the literature (Yang [16]; Ma and Hui [17]; Sattar [18]) for an unsteady parameter and for a constant wedge.

We outline the paper as follows. In §2, we present the formulation of the problem which includes defining the model and introducing a novel set of similarity transformations. Additionally we provide an exact solution of the UFSE for all pressure gradient and unsteady parameters. The Keller-box numerical solution of the unsteady problem is also given(For steady problem Kudenatti *et* al. [27]). For any choice of the these parameters, simulation of the required velocity profiles and corresponding wall shear stresses is relatively easy and straight forward to analyze. §3 devotes to study the asymptotic behavior far away from the wedge surface and for large unsteady parameter. In these cases, exact solutions of the linearized differential equations are given and subsequently analyzed. The final section summarizes the concluding discussions. Therefore the exact and asymptotic theories shall be developed for the unsteady problem that depends crucially on pressure gradient and as well as on wedge speed.

Nomenclature

u, v	velocity components in x and y-directions
ρ	Density
p	Pressure
β	Pressure gradient parameter
λ	Wedge speed
ν	Viscosity
k	unsteady parameter
Re	Reynolds Number
Re_x	local Reynolds number
ψ	Stream function
δ	Boundary layer thickness
erf	Error Function

Acronyms

B.C	Boundary Condition
BL	Boundary layer
2D	Two dimensional
UBL	Unsteady Boundary layer
UFSE	Unsteady Falkner-Skan Equation

2. Flow Theory and Analysis

Consider the 2D UBL flow of an incompressible fluid over wedge moving with a velocity $U_w(x,t)$ in the opposite direction to the outer free-stream velocity $U(x,t)$, and flow is in the half-space $y>0$. The x-axis is along and parallel to the wall of the wedge, and y-axis is normal to it. For these assumptions the Prandtl boundary layer equations

$$u_x + v_y = 0 \tag{2.1}$$

$$u_t + uu_x + vu_y = -\frac{1}{\rho}p_x + \nu u_{yy} \tag{2.2}$$

$$0 = p_y \tag{2.3}$$

For the flows with large Re, we have $|\frac{\partial u}{\partial y}| \gg |\frac{\partial u}{\partial x}|$. From (2.3), the pressure is a function of x only. Thus, the pressure gradient in (2.2) can be obtained (i.e. $u = U(x,t)$) as

$$-\frac{1}{\rho}(p_x) = U_t + UU_x \tag{2.4}$$

from the Bernoulli's theorem. The crucial point of the above simplification is that viscosity effects are completely neglected outside the flow i.e. $\nu = 0$ at $y = \delta$. From (2.2) and (2.4) we have that

$$u_t + uu_x + vu_y = U_t + UU_x + \nu u_{yy} \tag{2.5}$$

The B.C are

$$\begin{aligned} \text{at} \quad y = 0: \quad u = -U_w(x,t), \quad v = 0, \quad \text{and} \\ \text{as} \quad y \to \infty: \quad u = U(x,t) \end{aligned} \tag{2.6}$$

where $U_w(x,t)$ is the stretching surface velocity, and u merges with the mainstream unsteady flow U. The negative sign before $U_w(x,t)$ is due to the movement of both wedge and mainstream which are directionally opposite. When $U_w(x,t)$ is zero, both velocities vanish on the wedge surface (Sattar [18]). As noted earlier and following Batchelor [3], the BL thickness δ increases, from the point of first formation BL, continuously with distance x along the wedge surface. This is linked to how the acceleration or deceleration of the mainstream flow affects the BL thickness along the wedge surface. It is also expected that the wedge velocity U_w also varies as the mainstream flows. Therefore, both $U(x,t)$ and $U_w(x,t)$ take the form of the power-law relation and are given by

$$U(x,t) = U_\infty A(t) x^m, \qquad U_w(x,t) = U_{\infty w} A(t) x^m, \qquad A(t) > 0 \tag{2.7}$$

where both U_∞ and $U_{\infty w}$ are positive constants. In the present analysis $A(t)$ shall be discussed later in terms of k. In (2.7), m is force of the pressure gradient in the BL (cf (2.4) and (2.7)). The effects of different values of m on the boundary layer shall be discussed later. Note that, UBL equations (2.5) and (2.6) contain only two unknowns can be reduced to a single unknown function by defining the stream function $\psi(x,y,t)$ as

$$(u, v) = (\psi_y, -\psi_x) \tag{2.8}$$

(2.1) is automatically satisfied (2.5) becomes

$$\psi_{ty} + \psi_y \psi_{xy} - \psi_x \psi_{yy} = U_t + UU_x + \nu \psi_{yyy} \tag{2.9}$$

Further we take a new set of similarity variables as

$$\psi(x,y,t) = \sqrt{\frac{2\nu x U(x,t)}{1+m}} f(\eta), \quad \text{and} \quad \eta = \sqrt{\frac{(1+m)U(x,t)}{2\nu x}} y \tag{2.10}$$

which essentially reduce (2.9) to single dependent and independent variables. We emphasize that the above scaling for the is based on flow velocity distribution in the BLs in which BL exist and are *similar* for any x in the x-direction. In view of (2.7) and (2.10), (2.9) may be written as BL

$$f'''(\eta) + f(\eta) f''(\eta) + \beta(1 - f'^2(\eta)) = k\left(\frac{\eta}{2} f''(\eta) + f'(\eta) - 1\right) \tag{2.11}$$

and (2.6) become

$$f(0) = 0, \qquad f'(0) = -\lambda, \qquad f'(+\infty) = 1, \tag{2.12}$$

where $\beta = \frac{2m}{1+m}$ is the pressure gradient parameter,

$$k = \left(\frac{2}{m+1} \frac{U_\infty^{(m-2)}}{\nu^{m-1}}\right) \frac{A'(t)}{A^2(t)} \tag{2.13}$$

The $\lambda = \frac{U_{\infty w}}{U_\infty}$, the wedge surface has a specified velocity and stretch. The solution of (2.13) shall be discussed later. The $Re_x = \frac{U_\infty^{m-1} x^{m-1}}{\nu^{m-1}}$ it is assumed, to be $O(1)$ for the local Reynolds number, in the

derivation of (2.11). Here $\beta > 0$ (< 0) represents the accelerating (decelerating) flow. We emphasize on sign and value of λ, that is, when $\lambda = +1(-1)$, both mainstream and wedge velocities are moving with the velocity in the same (opposite) direction while for $\lambda > +\lambda_0(< -\lambda_0), \lambda_0 \neq 1$, where λ_0 is some value of λ, the wedge velocity is λ_0 times faster than the mainstream velocity but in the same (opposite) direction. Thus, the value generates a different class flows where the unsteadiness and pressure gradient are properly incorporated into the study. Further, the system (2.11) is a non-autonomous and not a stiff-differential equation.

We now construct a new class of similarity solutions of (2.11) and (2.12) that are related with the variation of pressure gradient and unsteady parameters. Although the system (2.12) and (2.13) may be solved numerically, we adopt a quite different approach for obtaining an exact solution of the problem. Indeed, we closely follow the exact procedure pioneered by Sachdev *et* al. [13] for the steady Falkner-Skan flow. In Kudenatti *et* al. [8], this method is successfully applied to obtain an exact solution of a class of steady Falkner-Skan BL flows which involves magnetohydrodynamic effects on the flow. On the other hand for stagnation point flow ($\beta = 1$), Kolomenskiy and Moffatt [1] have obtained a class of similarity solutions of both front and rear unsteady BL flows. They considered a wedge is not moving and solved the problem numerically for the range of k values for which solutions do exist.

We now move on to solve Unsteady Falkner-Skan equation (UFSE) (2.11) satisfying (2.12). We follow the similar procedure of previously studied steady case by Sachdev *et* al. [13] by incorporating the effects of unsteadiness into the method, and obtain all possible similarity type BL solutions.

A Riccati type of equation is obtained by Integrating (2.11) and (2.12) twice for $\beta = -1$ and $k = 0$ which has an exact solution

$$f(\eta) = \eta + \Delta - \frac{\Delta e^{-(\frac{\eta^2}{2} + \eta\Delta)}}{1 - \frac{\Delta}{2}\sqrt{\frac{\pi}{2}} e^{\frac{\Delta^2}{2}} (\mathrm{erf}(\frac{\eta+\Delta}{\sqrt{2}}) - \mathrm{erf}(\frac{\Delta}{\sqrt{2}}))} \tag{2.14}$$

where $\Delta = \pm\sqrt{-2(1+\lambda)}$ and $\mathrm{erf}(z) = \frac{2}{\sqrt{\pi}} \int_0^z e^{-\xi^2} d\xi$ is the error function. Note that when $\lambda > -1$, this is no longer a realistic condition, i.e. no solution exists, for $\lambda < -1$, there exist a dual solutions, while for $\lambda = -1$,

$$f(\eta) = \eta \tag{2.15}$$

is an exact solution of (2.11) and (2.12), and this shall be discussed later. Although in the present context Δ would need to be determined by the mainstream flow that is moving opposite to the wedge, ($\lambda < -1$) but mainly dominated by the wedge velocity .

In the rest of the paper, Δ restricts our analysis to one class of solution branch ($\lambda < -1$); and other branches of solutions will be considered in more detail in the asymptotic analysis. Yang and Chien [11] have derived the same solution of the steady Falkner-Skan equation in which λ is replaced by the mass transfer parameter, with similar restriction. We turn our attention now to obtain an exact solution to the system (2.11) and (2.12) for all k and β. To do this, rewrite (2.14) as

$$f(\eta) = \eta + \Delta - \frac{\Delta}{G(\eta)} \tag{2.16}$$

where

$$G(\eta) = \left(e^{-\frac{\Delta^2}{2}} + \sqrt{\frac{\pi}{2}}\frac{\Delta}{2}\mathrm{erf}\left(\frac{\Delta}{\sqrt{2}}\right)\right) e^{\frac{(\eta+\Delta)^2}{2}} - \sqrt{\frac{\pi}{2}}\frac{\Delta}{2} e^{\frac{(\eta+\Delta)^2}{2}} \mathrm{erf}\left(\frac{\eta+\Delta}{\sqrt{2}}\right). \tag{2.17}$$

The above simplification is obtained by addition and subtraction of the term $\frac{\Delta^2}{2}$ in the exponent of the numerator of (2.14) that makes a perfect square, then it is brought in $G(\eta)$ in (2.16). Substitution of (2.16) into the UFSE (2.11) and (2.12) leads to the following nonlinear equation

$$\begin{aligned} G^2G''' - G(6G' + \Delta - (\eta + \Delta - \frac{k}{2}\eta)G)G'' - (2\beta + k)G^2G' \\ + (\Delta(2-\beta) - ((2-k)\eta + 2\Delta)G)\,G'^2 + 6G'^3 = 0 \end{aligned} \tag{2.18}$$

and corresponding boundary conditions become

$$G(0) = 1, \qquad G'(0) = \frac{\Delta}{2}, \qquad G'(+\infty) = 0 \tag{2.19}$$

where $G = G(\eta)$. At this juncture, it is appropriate to mention that for $\beta = -1$ and $k = 0$, the solution of (2.18) and (2.19) is given by (2.17). Given nonlinear differential equation (2.18), the essence of exact solution is to express its solution by a proper base function. It is well know that a real solution $G(\eta)$ can be approximated using various different functions such as decaying exponential function, but we choose a relatively better base function from the exact analytical solution (2.17). That erf in (2.17) can be written in terms of the Taylor series expansion which have an infinite radius of convergence. Thus, series representation of these functions in (2.17) for $k = 0$ and $\beta = -1$ can be obtained which becomes a clue to get a similar series analysis for other values of β and k. Thus, we assume the base function as

$$G(\eta) = \sum_{n=0}^{\infty} a_n \eta^n \tag{2.20}$$

where a_n are to be determined. It should be emphasized that these coefficients a_n are functions of β and k and for $\beta = -1$ and $k = 0$, the above series (2.20) *exactly* matches the series representation of (2.17). As long as the series (2.20) converges, it must be the exact solution of (2.18) and (2.19), and because, it also embeds the exact solution (2.17) in it. We now focus on calculating all the coefficients a_n in (2.20). The first two coefficients $a_0 = 1$, $a_1 = \frac{\Delta}{2}$ are known from the boundary conditions (2.19) and substitution of (2.20) in (2.18) gives the recurrence relation

$$\begin{aligned}
a_{n+3} &= \frac{-1}{(n+1)(n+2)(n+3)}\Big(\sum_{j=0}^{n-1}\sum_{i=0}^{n-j}(j+1)(j+2)(j+3)a_i a_{n-j-i} a_{j+3} \\
&- \sum_{j=0}^{n}(\Delta(j+1)((j+2)a_{n-j}a_{j+2} + (2-\beta)(n-j+1)a_{j+1}a_{n-j+1}) \\
&- \sum_{i=0}^{j}(i+1)(j-i+1)(2\Delta a_{n-j} - 6(n-j+1)a_{n-j+1})a_{i+1}a_{j-i+1} \\
&+ \sum_{i=0}^{n-j}((j+1)(ja_{j+1} + \Delta(j+2)a_{j+2} - (2\beta + k(j+2)/2)a_{j+1})a_i a_{n-j-i} \\
&- (i+1)(6(j+1)(j+2)a_{j+2} + (2+k)(n-j-i)a_j)a_{i+1}a_{n-j-i})\Big)
\end{aligned} \tag{2.21}$$

for n = 1,2,3,- - -.
The above all coefficients a_n involve one free coefficient a_2.

In fact this a_2 is linked to the $f''(0)$ (can be obtained from (2.16) and (2.20))

$$a_2 = \frac{2f''(0) + \Delta^3}{4\Delta}. \tag{2.22}$$

Thus, it is equivalent to obtain a value of either a_2 or $f''(0)$ such that the end condition in (2.19) or in (2.12) is automatically satisfied. This is quite challenging and crucial part of the calculation. To compute a_2 (or $f''(0)$), integration of the UFSE (2.11) over the flow domain gives

$$\int_0^{\infty}(f'(\eta) - \frac{k}{2}f'(\eta) - f'^2(\eta))d\eta + \beta\int_0^{\infty}(1 - f'^2(\eta))d\eta = f''(0) - \frac{k}{2}\eta_{\infty} \tag{2.23}$$

where η_{∞} denotes the large value of η. While deriving (2.23), it has been assumed that for given k, the term $\eta f''(\eta) \to 0$ as $\eta \to \infty$. The numerical study of Riley and Weidman (1989) [12] and in most of the other investigations has confirmed this tendency, also in the present case $\eta f''(\eta) \to 0$ more faster than

$f''(\eta)$ alone as $\eta \to \infty$. This ensures a faster convergence of the series. We now write (2.23) in more convenient manner is written as

$$\int_0^{\eta_\infty} (f'(\eta) - \frac{k}{2} f'(\eta) - f'^2(\eta)) d\eta + \beta \int_0^{\eta_\infty} (1 - f'^2(\eta)) d\eta = f''(0) - \frac{k}{2}\eta_\infty. \tag{2.24}$$

Looking at equation (2.24), $f'(\eta)$ term (cf (2.16), (2.20), (2.22)) involves $f''(0)$ and thus, $f''(0)$ is in LHS and RHS. It is advisable to obtain $f''(0)$ iteratively with suitable initial approximation for $f''(0)$. Fortunately, the computation of (2.24) provides a sufficient freedom to choose initial approximation for $f''(0)$, required number of coefficients a_n (2.20) and the value of η_∞ of (2.24). This kind of great freedom ensures the ease of computation of (2.24). Note that numerous initial conditions for $f''(0)$ were performed which is computationally expensive for all values of β and k as convergence of the series was often slow except for the case $\beta = -1$ and $k = 0$. Instead, an initial guess for $f''(0)$ is chosen that is obtained from (2.11) and (2.12) for $\beta = -1$ and $k = 0$. This guess ensures the speedy convergence of the series and reduces the number of iterations drastically in the above integration. During the integration process in (2.24), whenever the convergence is slow, the Padé technique (Bender and Orzag [20]) is regularly used to broaden the domain of convergence and enhance converge rate of the series. Generally, we have used the diagonal Padé approximant to sum the series (2.20). We obtain $f''(0)$. For similar detailed computations of (2.24), see Kudenatti *et* al. [8]. Once the numerical value of $f''(0)$ is obtained, the coefficient a_2 and thus all a_n in (2.21) are completely known and hence the series $G(\eta)$ in (2.20). Therefore, the proposed form (2.16) is now completely an explicit solution in terms of convergent series form. Therefore, we have obtained an exact solution of the UFSE (2.11) and (2.12) for all β and k which is

$$f(\eta) = \eta + \Delta - \frac{\Delta}{G(\eta)} \tag{2.25}$$

where $G(\eta)$ is convergent series given by (2.25). Therefore, the nonlinear UFSE (2.11) with boundary conditions (2.12) contains rather rich mathematical structure and simple analysis. As long as the series solutions (2.25) is convergent, where $G(\eta)$ is governed by (2.20), it must be an exact solution of the nonlinear problem (2.11), the present form (2.25) includes many of the previously considered numerical investigations (for steady case Riley and Weidman [12]; Kolomenskiy and Moffatt [1] for stagnation point flows, etc) as a special case. The above form is extensively used to plot the velocity profiles and also to obtain $f''(0)$. The solution (2.25) is used to interpret the effects of mainstream forcing in terms of pressure gradient and unsteady on the BL flow. Thus, meaningful comparisons of similarity solutions obtained from (2.25) and the direct numerical solutions are always possible. In addition, to supplement the results of (2.25) for various parameters involved in it, we have also performed asymptotic analysis of the system (2.11) and (2.12) for far-field behavior and large k (which are given in the next section).

Although in the present context, the pressure gradient β and unsteady k are entirely at our disposal, but in BL computations these parameters would define the nature of the flow that is whether the flow is accelerated or decelerated, this depends on a sign of β and k.

In another approach we solve the UFSE numerically using the Keller-box method. The error tolerance was set to 10^{-6} for all parameters discussed. To be specific, $f''(0)$ is checked for accuracy for all parameters when the velocity profile is produced. Keller-box code is used to compliment and compare our exact solutions. Next we analyze the results obtained from (2.25). To validate the efficiency of the method and the accuracy of the results, the $f''(0)$ are computed first and are cross checked for various values of β, k and λ. Table 1 shows the results are in excellent accord with each other. To obtain these results, the series $G(\eta)$ has taken less number of coefficients and has a good domain of convergence. The accuracy of $G(\eta)$ has taken less number of coefficients and has a good domain of convergence. The accuracy of the results shown in table 1 verifies validity of the method, and from a mathematical point of view, this is a smart way to solve the UFSE problem. Further, we also observe that the $f''(0)$ increases (in absolute sense) for increasing parameters. We now discuss how the pressure gradient affects the BL behavior can be explained in terms of the velocity profiles.

A further important discussion is on the effect of pressure gradient (both accelerated and decelerated) on the unsteady BL flows. A good comparison of steady and unsteady flow demonstrates the major

qualitative differences on flow patterns when pressure gradient is varied (for $k = 0$ the steady case is well-studied). More recent papers on unsteady BLs have focused on stagnation point flow ($\beta = 1$) and results are well established, and hence discussion on it is no longer required. However, we always compare and reduce our results for various values of β with stagnation point flows. Figure 2a shows the velocity profiles $f'(\eta)$) for various values of β and for $k = 1$ and $k = 2$ (accelerated flows). Note that as β increases, the unsteady flow in mainstream area beyond the boundary layer, the flow is directed toward the wedge surface, resulting in a thinner boundary layer. As k continues to increase, the unsteady flow is completely carried toward the wedge surface. In any case, the flow is always accelerated (also discussed partially by Kolomenskiy and Moffatt [1]. Some of the velocity distribution for negative k ($k = -1$ and $k = -2$) are plotted in figure 2b for the same values of β. The similar trends are observed for these parameters. Thus, the effects of β and k on the unsteady BL flow are clearly seen. Note that the exact solution (2.25) has a convergent series in fact throughout the flow domain, meaning that for $\beta > 0$, and $\pm k$, the series is always convergent. The effects of pressure gradient are more predominant than unsteady on the BL. When β is decreased below zero (decelerated flow), in figure 2c, we show the flow velocity distribution in the BL s that are calculated from (2.25) with $k = 1$ and $k = -1$ (here solid lines are for $k = 1$ and dashed lines are for $k = -1$). We observe from this figure that except for the case $\beta = 0$ (wherein both profiles are attached to the wedge surface), for other β, the results are obtained from (2.25) but the series $G(\eta)$ has more number of coefficients than figure 2a-2b results, in addition, the BL region is also slightly large but this did not hinder the convergence of the series. Further, for decelerated flow, the profiles are generally oscillatory in nature (i.e. the curves have both under-shoots ($f'(\eta) < 1$) and over-shoots ($f'(\eta) >1.4$) for some η, although these are difficult to observe experimentally (these results will be further confirmed by the asymptotic solutions). As in the case of steady flow (Oskam and Veldman [14]; Hastings and Troy [10] these oscillations are observed in unsteady BL flow as well; these oscillations are more for negative values of $k(= -1)$ than positive k. But finally they smoothly approach the mainstream flow validating the form (2.25) for negative β. These results are continued to exist even for other values of λ and are shown in figure 3 when both k and β are varied and held negative. Surprisingly, the UFSE (2.11) exhibits dual solutions for some $\beta(< 0)$, with the additional solution being more oscillatory as seen clearly in these figures. We observe an uncommon interesting characteristic nature between figure 2 and figure 3. For an adverse pressure gradient ($\beta < 0$), the oscillations are likely to occur in the BL irrespective of whether k is positive (small) or negative; which would plausibly cause the BL separation when β is decreased further, whereas these oscillations disappear for a favorable pressure gradient ($\beta > 0$) as seen in figure 2. These oscillations leading to BL separation can also be avoided by adding mass transfer to the existing model and also by involving external force like magnetic field which would be a future subject interest.

Thus, the conclusion is that the solution (2.25) is an exact solution of the UFSE (2.11) that satisfies the boundary conditions (2.12) for variable pressure gradient and unsteady parameters wherein the base function $G(\eta)$ given by (2.20) is always convergent series. In this series, the number of coefficients a_n that are required to compute the $f''(0)$ and corresponding flow velocity distribution in the BL s $f'(\eta)$ depend on the sign of β and k. As discussed in previous para when $\beta > 0$, the number of coefficients in the series is quite less to have convergent solution whereas the case of $\beta < 0$ is different, i.e the number of coefficients for the series to converge is quite large. In any case convergence of the series and domain is not affected by the number of coefficients. Region of validity of the solution is enhanced by means of the Padé technique. The present method easily helps in computing the $f''(0)$ and the velocity distribution in the BL at a stretch.

3. Asymptotics

In the remainder of the paper, we concentrate on asymptotic behavior of (2.11). Firstly, the aforementioned exact results are completely justifiable from the asymptotic results. The above results clearly indicate that solutions behave linearly far away from the wedge surface. Therefore, it is prime concern to obtain the similarity solutions of linearized unsteady Falkner-Skan equation for $\eta \gg 1$. Secondly on the other hand, when k is large, the unsteadiness completely dominates over the BL flow than the inertial forces alone, hence latter forces can be neglected. Therefore, these special cases give a good deal of simplifications in the full nonlinear system (2.11). These cases are considered in the below subsections.

3.1. Far-field behavior:

The boundary condition at the edge of the BL suggests to look for the existence of similar solutions for all parameters by investigating the large η asymptotics, i.e. $\mid f'(\eta)-1 \mid \ll 1$ as $\eta \to \infty$. Consequently the ideas of previous work (Kudenatti *et al.* [8], [9], [26] for steady case) and also from the results of previous section, we define the new stream function $E(\eta)$ as

$$f(\eta) \sim \eta + I_c + \int E(\eta) d\eta \tag{3.1}$$

where $E(\eta)$ and all its derivatives are assumed small and I_c is an integration constant (in the present case $I_c = 0$ because of (2.12)). Substituting $f'(\eta) = 1 + E(\eta), f''(\eta) = E'(\eta), f'''(\eta) = E''(\eta)$, in (2.11) and (2.12) and upon linearization, the system leads to the following equation

$$E''(\eta) + \left(\frac{2-k}{2}\right)\eta E'(\eta) - (2\beta + k)E(\eta) = 0 \tag{3.2}$$

and boundary conditions

$$E(0) = -(1+\lambda), \quad E(\infty) = 0. \tag{3.3}$$

Note that the unsteady parameter k plays a crucial role, and gives two very different mathematical solutions. The system (3.2) and (3.3) for k = 2, the solution is

$$E(\eta) = -(1+\lambda)e^{-\sqrt{2(1+\beta)}\eta} \tag{3.4}$$

for $\beta > -1$. For $k \neq 2$, the complete solution is given by

$$E(\eta) = \sqrt{\frac{k_1}{2}}\ (1+\lambda)\ k_2 \eta \mathcal{M}\left(\frac{1}{2}+k_3, \frac{3}{2}, -\frac{k_1}{2}\eta^2\right) - (1+\lambda)\mathcal{M}\left(k_3, \frac{1}{2}, -\frac{k_1}{2}\eta^2\right) \tag{3.5}$$

where $\mathcal{M}(\cdot,\cdot,\eta)$ is the confluent hypergeometric function of first kind (Abramowitz and Stegun [21]; Andrews [22]) and $k_1 = 1 - \frac{k}{2}$, $k_2 = \frac{2\Gamma(1-k_3)}{\Gamma(\frac{1}{2}-k_3)}$, $k_3 = \frac{2\beta+k}{k-2}$. As discussed in § 2, for $\lambda = -1$, the solution of (3.2) affirms the trivial solution $f(\eta) = \eta$ that demarcates the solution structure. When $\lambda > -1 (\lambda < -1)$ the flow velocity distribution in the BL s approach their asymptotic value unity (the boundary condition) from below(above). Thus before plotting the flow velocity distribution in the BL s $f'(\eta)$ using (3.1) with (3.5), we make some analytical conclusions on the asymptotic dependence of the flow parameters on the confluent hypergeometric functions. For this, taking the large η asymptotics for $\mathcal{M}(\cdot,\cdot,\eta)$, (Abramowitz and Stegun [21]) with appropriate first and second arguments in (3.5), and simplifying, we get

$$E(\eta) \sim \underbrace{c_{11} Z^{-k_3}}_{I} + \underbrace{c_{22} e^{-Z} Z^{-\frac{(2k_3+1)}{2}}}_{II} \tag{3.6}$$

where

$$\begin{aligned} Z &= \frac{k_1\eta^2}{2}, \quad c_{11} = (-1)^{-k_3}\left(\frac{(1+\lambda)\sqrt{\pi}}{\Gamma(\frac{1}{2}-k_3)}\right), \\ c_{22} &= (-1)^{-k_3}(1+\lambda)\left(\frac{\sqrt{\pi}\ \Gamma(1-k_3)}{\Gamma(\frac{1}{2}+k_3)\Gamma(\frac{1}{2}-k_3)} - \frac{\sqrt{\pi}}{\Gamma(k_3)}\right). \end{aligned}$$

Therefore, the following observations can be drawn:

1. When $k > 2$: from (3.6) we have I decays to zero algebraically as Z^{-k_3} for $\beta > -1$, in this case the minimum mainstream flow behavior is proportional to $A(t)x^{-\frac{1}{3}}$ and II diverges exponentially. Then the solution (3.5) of (3.2) is unique.

2. When $k < 2$ and $\beta \geqslant 0$: we have that as I diverges algebraically as $Z^{+constant}$ and the only convergent solution is II. On the other hand when $\beta < 0$, we have both convergent solutions and decay to zero, in this case flow is always decelerated.

3. When $k < -2$ and $\beta \leq 1$: the exponent in both solutions I and II remains negative and thus decay to zero, in fact very slowly. In this case the solution (3.5) of (3.2) is unique. Furthermore, when $\beta > 1$, we see that I diverges algebraically as $Z^{+constant}$, and II decays slowly to zero.

In addition to the above results, we will also study the nature of the flow velocity distribution in the BL s from the asymptotic solutions, and these solutions always compliment the exact solutions. This study also indicates that the flow becomes more attached to the wedge surface for increasing positive values of β. This is clearly seen in figures 4a-4b for various values of λ and k. Further, the flow becomes oscillatory type for negative values of β as is seen in figures 4c-4e. In particular, figures 4c-4d show a clear distinction between accelerated BL ($\beta > 0$) and oscillatory type BL ($\beta < 0$). For decreasing β, figure 4d shows the flow oscillates number of times before reaching the mainstream condition. These results agree well with some of the previously published results for steady BL flow (Hastings and Troy [10]; Oskam and Veldman [14]; more recently Kudenatti *et* al. [8]). Taking the effects of pressure gradient into account, probably this type of flows in unsteady BL are rather new since the only discussed case is stagnation point flow ($\beta = 1$). Duck and Dry [23] have certainly reported that oscillatory type flows are common for some extreme values of β. This trend of being oscillatory is tested for different wedge speed (λ), and found that results are similar. These linear solutions show significant alterations of the nature of the flow, and also they definitely correlate them to available exact solutions. Further evidences about the flow oscillations come from both analyses (§ 2 and § 3) that an existence of oscillations is due to an unsteady flow influenced by adverse pressure gradient which may give rise to decelerated flow close to the wall, this makes velocity to decrease. However, this tendency is reversed away from the wall because the kinematic viscosity decreases eventually flow velocity distribution in the BL increases.

3.2. Asymptotics for large k:

In the previous section (§ 2), the exact solutions to the UFSE (2.11) are obtained for all values of k and β including large k. In addition to the far-field behavior results of the UFSE, it is appropriate to look for large k asymptotic for the UFSE (2.11) which helps to compare exact solutions for large k. The existence of these unsteady solutions is fairly uncommon, and thus may be regarded as an alternative to the exact solutions for large k. A further aim of the present paper is to attempt to give the various possible solutions to the UFSE for large k. When k is large and positive it is reasonable to neglect nonlinear convective acceleration in (2.11) in comparison with linear diffusive acceleration, and this obviously leads to the linear UFSE

$$H''(\eta) - \frac{k}{2}\eta H'(\eta) - kH(\eta) = -(\beta + k) \tag{3.7}$$

and the corresponding boundary conditions (2.12) become

$$H(0) = -\lambda, \qquad H(+\infty) = 1 \tag{3.8}$$

where $H(\eta) = f'(\eta)$ is taken without loss of generality. The effects of unsteady and pressure gradient on BL flow do not vary as $k \to +\infty$. Solution of (3.7) that satisfies (3.8) is given by

$$H(\eta) = -\lambda + \frac{\sqrt{k\pi}}{2}\left(\lambda + \frac{\beta + k}{k}\right)\eta e^{K^2}\operatorname{erfc}(K) \tag{3.9}$$

where $\operatorname{erfc}(K) = 1 - \operatorname{erf}(K)$ is complementary error function (Abramowitz and Stegun [21]) and $K = \frac{\sqrt{k}}{2}\eta$. Also note that

$$\int_K^\infty e^{-\zeta^2} d\zeta \sim \frac{1}{2K} e^{-K^2} + O(K^{-3}) \quad \text{as} \quad K \to \infty \tag{3.10}$$

has been used while deriving the solution (3.9). Note also that (3.9) is a unique solution of (3.7), and sign of k should be always positive. Thus, with these we now consider the $f''(0)$ $H'(0)$ (corresponds to

$f''(0)$), that are given in figure 5 along with exact solutions obtained from (2.25). The results of (3.9) in figure 5 are plotted for $k \geq 5$ and the values of λ and β are mentioned in it. The results obtained from (3.9) are found to be qualitatively agreeing well with those produced from (2.25). This class of results is important from a theoretical point of view, in particular, we make the following general observations:

1. in each case (for each $f''(0)$), the velocity profiles exists;

2. a linear decrease in $f''(0)$ for increasing k;

3. large k asymptotic results are embedded in exact solution.

Some discussion of the class of flow velocity distribution in the BL s for β, k and λ has been given in the previous section. A close observation gives a hint that the $f''(0)$ becomes zero for certain values of k either positive or negative predominantly depending on pressure gradient and also on λ. For example, $\beta = -0.5$ it vanishes at $k = -0.419512$, $\beta = -1.5$ it vanishes at $k = 3.797423$. When β is held positive constant, $f''(0)$ becomes zero for negative and large k. For $\beta = 0.5$ and $\beta = 1.5$, vanish of the $f''(0)$ is found at $k = -5.269820$ and $k = -10.121101$ respectively. Also at $\beta = -0.586557$, both k and $f''(0)$ become zero, reducing the present problem to the steady two-dimensional BL flow. The exact reasons for vanish of the wall stress for various λ are still not known. On the other hand, we also experimented to obtain asymptotics for large and negative k to compare our results with exact solutions but ended without success. The fundamental problem encountered was the sign of k, hence (3.7) leads to one-parameter family of solutions.

4. Figures and Tables

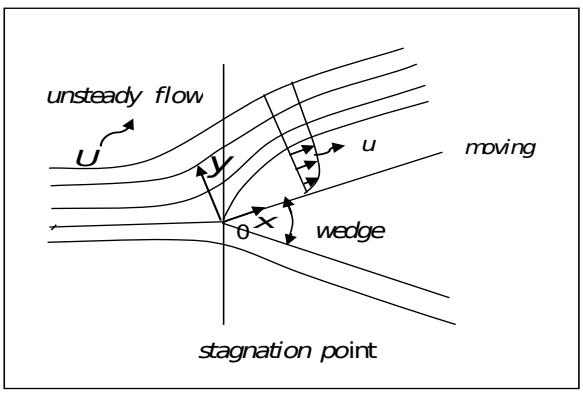

Figure 1: The physical model is displayed in the schematic flow configuration. The BL is overtaken by the unsteady mainstream flow U. The symmetric BL is created by the included angle $\frac{\beta\pi}{2}$'s moving wedge. The stagnation point flow and the flow over a flat plate are represented by the situations $\beta = 1$ and $= 0$, respectively.

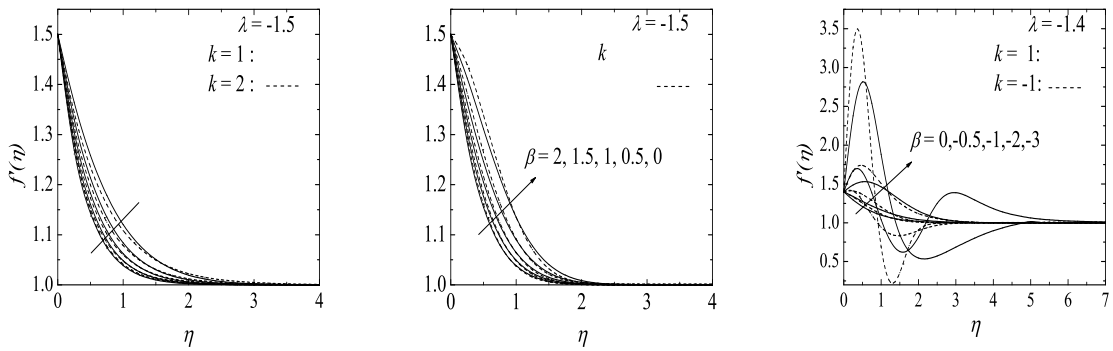

Figure 2: Variation of flow velocity distribution in the BLs $f'(\eta)$ with η for various values of β, λ, k. Note that $f'(0) = -\lambda$. The arrow marked lines show decreasing values of β. These profiles clearly indicate the effects of pressure gradient on the BL flow.

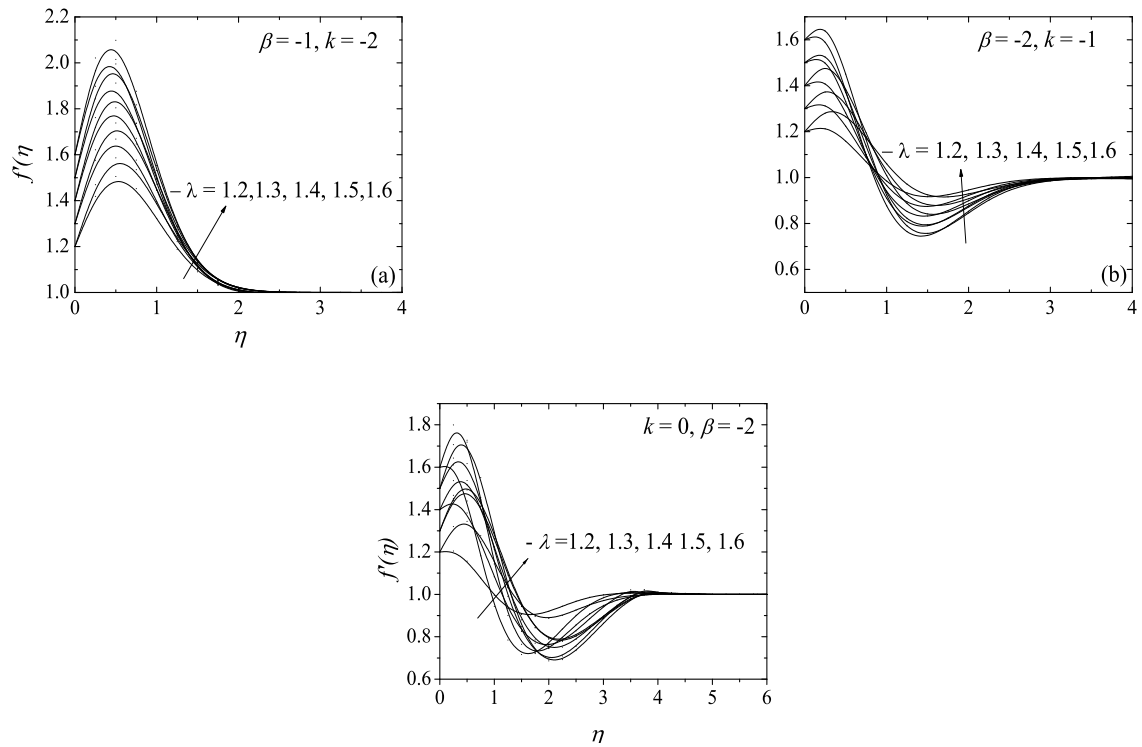

Figure 3: Plot of flow velocity profiles for different values of λ, β and k. Note that $f'(0) = -\lambda$. In figure (c), for steady flow ($k = 0$), the curves approach their end-condition very slowly.

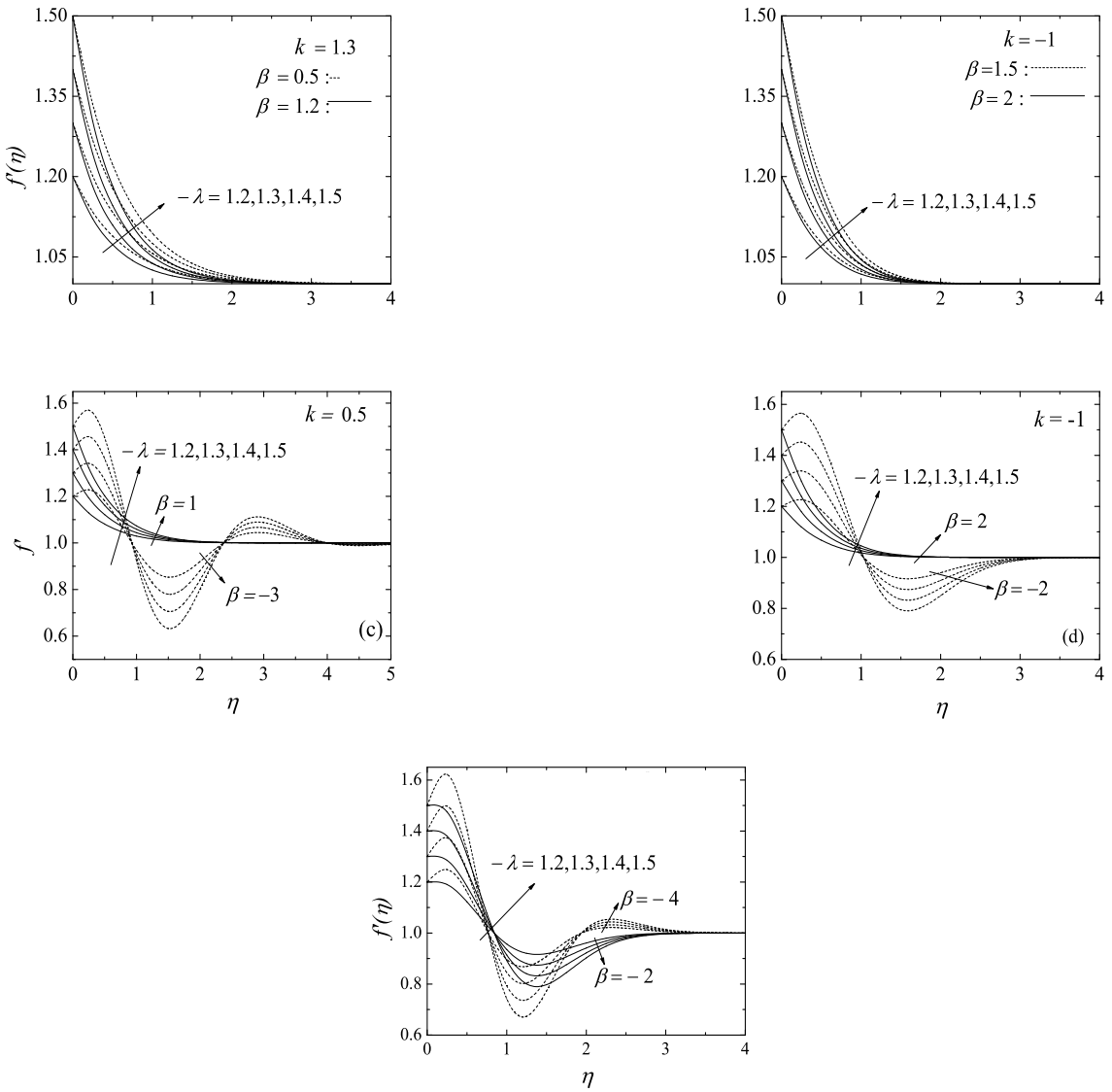

Figure 4: Asymptotic solution for different λ, β and k. Note that $f'(0) = -\lambda$. These curves show fast convergence to 1 as $\eta \to \infty$.

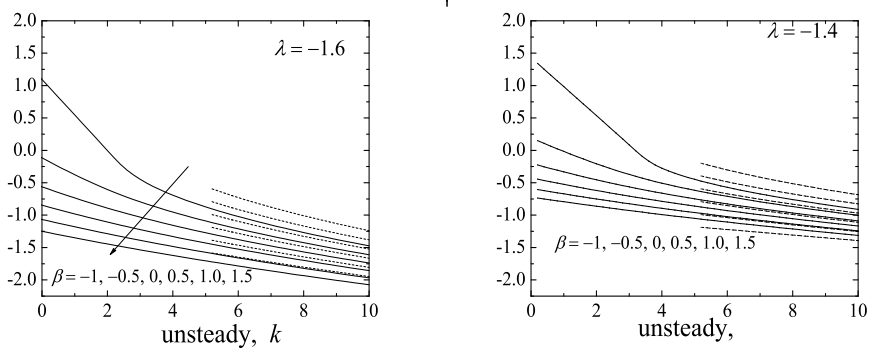

Figure 5: An example of how the velocity gradient at the wall changes for various values of β and λ with respect to the k and exist for all these values. An arrow-marked line displays growing β values. The dashed lines represent the asymptotics for $k \geq 5$ for $H'(0)$ $(f''(0))$. For any of these parameters, the flow velocity distribution in the BL s exist. A line with arrow mark shows increasing values of β. The dashed lines are for $H'(0)$ $(f''(0))$ asymptotics which are drawn for $k \geq 5$.

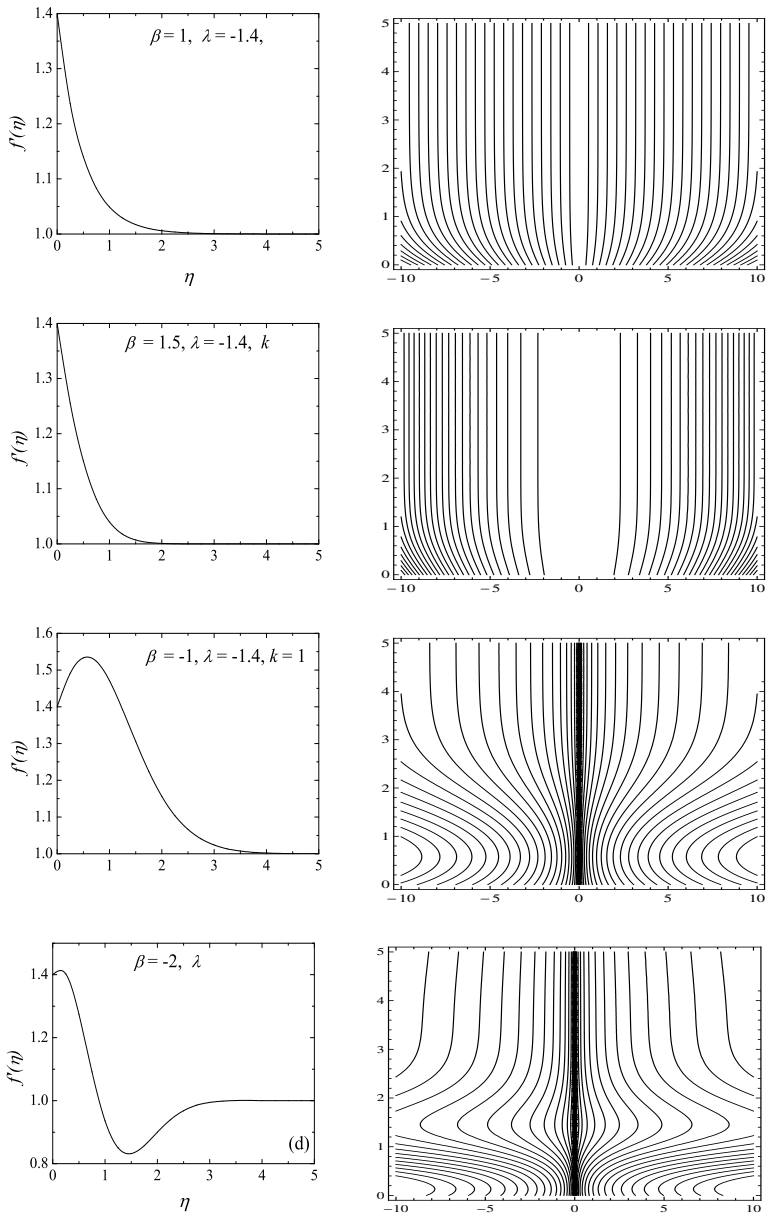

Figure 6: Variation of flow velocity distribution in the BLs $f'(\eta)$ with η (left column)and corresponding streamline patterns (right column) for various values of λ, β, and k. In these streamlines, the vertical line is η and the horizontal line is taken as x.

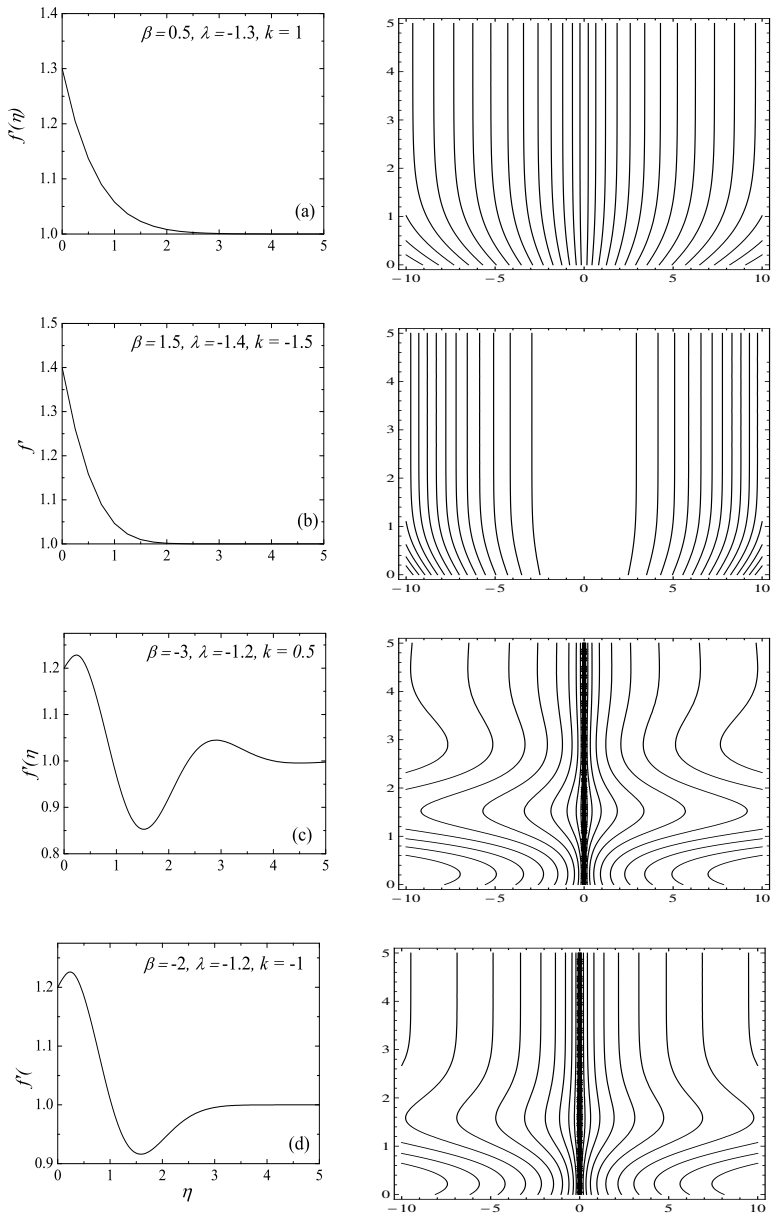

Figure 7: Variation of flow velocity distribution in the BLs $f'(\eta)$ with η (left column) and corresponding streamline patterns (right column) that are obtained by asymptotic solution for different values of λ, β, and k. In these streamlines, the vertical line is η and the horizontal line is taken as x.

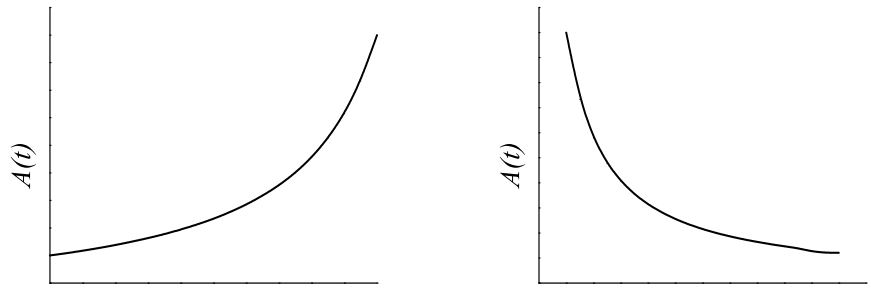

Figure 8: (a) accelerating flow (b) decelerating flow are Time Evolution of the flow strength $A(t)$

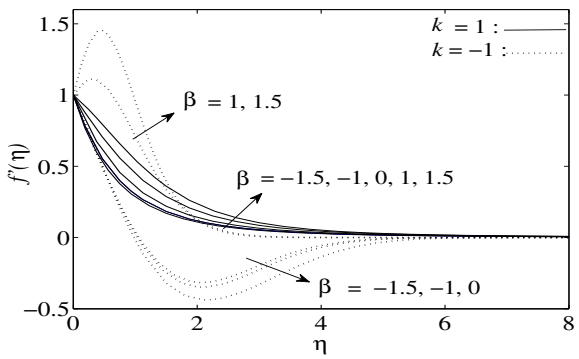

Figure 9: Decaying solutions for $f'(\eta)$ for nonlinear stretching rate parameter.

5. Conclusion

In this paper the similarity solutions for the unsteady Fakner-Skan equation have been obtained when the mainstream flow of the form $A(t)x^m$ is driven. We have studied the dependency of BL flow on three parameters: β measuring the pressure gradient, k measuring the unsteady of the flow and λ measuring the precise wall stretch and speed of the wedge surface. The new approach has been developed (originally developed for steady case: Sachdev *et* al. [13] along with the asymptotics (for large k and η) and the finite difference based Keller-box numerical technique (to compare the results presented in this paper). These results exist for all β, k and λ and include the stagnation point flow results (the only case studied previously). These solutions are, in fact, the exact solutions of the full Navier-Stokes equations in the BL limit. For all parameters the velocity component becomes linear as asymptotically satisfying the zero-shear viscosity limit for $\eta \gg 1$.

In particular, an exact solution of the UFSE (2.14) for $\beta = -1$ and $k = 0$ is obtained and it is modified to get all the solutions for β and k in convergent series form. The solutions corresponding to $\beta < 0$ are particularly interesting and rather challenging since these results are oscillatory type and hence series has a slow convergence. In this situation we have taken more number of coefficients a_n in the series (2.20). But this is not the case for $\beta > 0$ wherein very fewer coefficients a_n have been taken. In both cases, the Padé approximants (Bender and Orzag [20]) have been used to sum the series that enables to extend the convergent domain. The Domb-Skyes plot again confirms this flow domain within which the velocity profiles satisfy the zero-shear viscosity condition for $\eta \gg 1$.

Further, to validate the exact solution (§ 2), we also have obtained the asymptotic solution of the UFSE (2.18) in the limit of $\eta \to \infty$ and $k \to \infty$, and results are qualitatively comparable to exact

solutions, and to those of Sachdev *et* al. [13] for steady case. Note that the latter asymptotic results are special exhibiting the unique feature of the UFSE for $k \to \infty$. In figure4 we have plotted these results but these results are not valid for $k \to 0$. For $k \to 0$, the solutions largely deviate from the exact and numerical results clearly indicating nonphysical approximation we have made while deriving these asymptotic solutions. The mathematical reason for these nonphysical results is due to the neglect of the nonlinear convection terms in (2.18), and for small k, these terms are important to produce the correct the velocity profile in the BL. Nevertheless the exact solutions obtained from (2.25) are valid for all k including small and large k, and also embeds the solutions of (3.9). Therefore the solution (2.25) preserves the asymptotic results for large k, thereby making (2.25) more analytical in nature. On the other hand, when k is fairly large (3.9) gives a better way to compute the velocity profiles (with slight deviation). Thus, since we are mostly interested in computing the velocity profiles $f'(\eta)$, our present approach is extremely efficient with desired accuracy and with the correct asymptotic limits, and also taking into account all parameters investigated.

As discussed previously, the similarity variables (2.10) exist on the basis that there is similar velocity profile for each x in the streamwise direction. This needs to be validated from our results, and thus, in figures 5 and 6 some of the velocity profiles and corresponding pattern of streamlines (contour plots) are plotted as function of η and x from our exact and asymptotic solutions for various parameters (described in figures). In both cases these patterns are plotted with $\nu = A(t) = U_\infty = 1$. The velocity profiles in the BL could be realized from these streamline patterns that validate the existence of the similarity solutions. In particular, from these figures, it is very clear that there is a velocity profile for each x. Depending on the nature (whether accelerated or oscillatory type) of the velocity profiles, corresponding streamlines also represent the similar nature of the flow for each x. Also a close inspection of these figures illustrates that the flow pattern in the streamlines can be roughly divided into two regions: the near field where the flow is mainly dominated by the viscous effects, and the far-field where it is more controlled by the mainstream flow(inviscid flow). The thickness of the BL depends on the magnitude of both unsteadiness and the pressure gradient. For positive β, the streamlines in the unsteady BL are essentially pulled towards the boundary by the wedge surface. Similarly for negative β, flow is oscillatory type near the surface, and away from it, it follows the mainstream forces. These streamlines also eventually satisfy the zero-shear viscosity condition as $\eta \to \infty$ (i.e. $f'(\eta) \to 1$ as $\eta \to \infty$). These patterns of the streamlines from exact solutions and asymptotic solutions complement each other.

It is important to note that as stated earlier, k is the dimensionless unsteady parameter and is a constant for given pressure gradient β. For $k \neq 0$ ($k = 0$ is the steady flow), the solution of (2.13) is given by

$$A(t) = \frac{C_1}{C_1 t_0 - kt} \tag{5.1}$$

where t_0 is the constant of integration such that $A(0) = \frac{1}{t_0} > 0$, and $C_1 = \left(\frac{U_\infty^{(3\beta-4)}}{\nu^{2(\beta-1)}}\right)^{\frac{1}{2-\beta}} (2-\beta)$. Note that the solution $A(t)$ has a finite time singularity at $t = \frac{C_1 t_0}{k}$. This finite-time singularity value increases for $k > 0$ when $\beta \to -\infty$, in this case the flow becomes accelerated. For adverse pressure gradient ($\beta < 0$) the singular value decreases for $k < 0$. The solution $A(t)$ is plotted in figure 7 for both accelerated and decelerated flows for some representative values. In either case, the similarity solutions exist and have a BL character. This trend is observed for all values of β and k.

The various numerical computations are carried out in order to validate if the self-similarity solutions are realized with a particular form for $A(t)$ in (2.7) and in subsequent analysis. The model under consideration is a two-dimensional laminar viscous flow over a stretching sheet in which the outer unsteady velocity is reduced to zero and the wedge surface velocity is kept fixed. The velocity field develops due to the stretching of the sheet with velocity proportional to the power of distance and with nonlinear stretching rate. In this case BL grows upstream from the leading edge, and a solution to the BL still exists. When the sheet is stretched impulsively at $t = 0$, then its velocity equals the outer unsteady velocity

$$U(x,t) = U_w(x,t) = U_\infty A(t) x^m \tag{5.2}$$

with unsteady function assuming the from (Fang *et* al. [24])

$$A(t) = \frac{1}{1 - U_0 t} \tag{5.3}$$

where U_0 is a positive constant. Thus, the governing equation describing the above model takes the form

$$f''' + ff'' - \beta f'^2 = k(\frac{\eta}{2} f'' + f') \tag{5.4}$$

with boundary conditions

$$f(0) = 0, \qquad f'(0) = 1, \qquad f'(\infty) = 0. \tag{5.5}$$

The Keller-box method is re-coded for the above system for various nonlinear stretching parameter β and unsteady parameter k, and some of the velocity profiles for the accelerating and decelerating flow are given in figure 8. The profiles approach the end condition on both sides of the stretching sheet surface. The accelerating flow profiles converge faster than decelerating flow profiles. As before, in the decelerating flow, we find the profiles have inflection points, but finally flow the evolves to its self-similar shapes.

Our simulations on two-dimensional unsteady flow illustrate that the velocity profiles behavior is driven mainly by the pressure gradient, and in the BL region flow becomes oscillatory for adverse pressure gradient. Though the results of β and k presented here confined to the fundamental solution that approach $f'(\infty) = 1$ monotonically, a potential investigation of these oscillatory solutions would provide a rich subject for further study. One possible additional would be to consider the effect of magnetic field, suction and injection on the unsteady BL flow with mass transfer.

$\beta = -2$	$k = -1$		$k = 0$		$k = 1$	
λ	Exact	Numerical	Exact	Numerical	Exact	Numerical
-1.2	0.197541	0.198590	0.624292	0.624292	1.309164	1.309165
-1.3	0.267697	0.267697	0.822137	0.822137	1.601108	1.601116
-1.4	0.331632	0.331770	0.990208	0.990208	1.842560	1.842560
-1.5	0.395045	0.387527	1.138620	1.138620	2.056840	2.056870
-1.6	0.435924	0.436628	1.273126	1.273126	2.240998	2.240998
$\beta = 1.5$						
λ	Exact	Numerical	Exact	Numerical	Exact	Numerical
-1.2	-0.352619	-0.352619	-0.390005	-0.3900134	-0.425442	-0.425442
-1.3	-0.540177	-0.540190	-0.595244	-0.595244	-0.647527	-0.647527
-1.4	-0.734955	-0.734955	-0.806618	-0.807050	-0.874941	-0.875671
-1.5	-0.936693	-0.936693	-1.024190	-1.025269	-1.109739	-1.109739
-1.6	-1.145214	-1.145214	-1.249738	-1.249746	-1.349577	-1.349618

Table 1: Comparison of wall stress value $f''(0)$ obtained from (2.16) with numerical solution of the problem.

Acknowledgments

The authors would like to thank the referees for their valuable comments and suggestions, which helped me to improve the quality and clarity of this paper.

References

1. Kolomenskiy D, Moffatt H . K. *Similarity solutions for unsteady stagnation point flow*, J. Fluid Mech. **711** (2012) 1-17. (http://dx.doi.org/10.1017/jfm.2012.397)
2. Kolomenskiy D, Moffatt H. K, Farge M, Schneider K. *The Lighthill-Weis-Fogh clap-fling-sweep mechanism revisited*. J. Fluid Mech. **676**, (2011) 920110 572-606. (DOI:10.1017/jfm.2011.83)
3. Batchelor GK. 1967 *An introduction to fluid dynamics*. Ist edition. Cambridge University Press (1967).
4. Schlichting H, Gersten K *BL Theory* 8th edition. Springer, Newyork,(2000) .
5. Hiemenz K. *Die Grenzschicht an einem in den gleichförmigen Flüssigkeitsstrom eingetauchten geraden Kreiszylinder*. Dingl. Polytech. J. **326**, (1911) 321-410.
6. Dhanak M. R, Duck P. W. *The effects of freestream pressure gradient on a corner BL*. Proc. R. Soc. Lond. A **453**, (1997) 1793-1815. (DOI:10.1098/rspa.1997.0097)
7. Duck P. W, Stow S. R, Dhanak M. R. *BL flow along a ridge: alternatives to the Falkner-Skan solutions*. Phil. Trans. R. Soc. Lond. A **358**, (2000) 3075-3090. (DOI:10.1098/rsta.2000.0697)
8. Kudenatti RB, Kirsur SR, Achala LN, Bujurke NM. *MHD BL flow over a non-linear stretching boundary with suction and injection*. Int. J. Non-linear Mech. **50**, (2013) 58-67. (DOI:10.1016/j.ijnonlinmec.2012.11.005)
9. Kudenatti RB, Kirsur SR, Achala LN, Bujurke NM. *Exact Solution of two dimensional MHD boundary layer flow over a semi-inifinte flat plate*. Non-linear Sci. and Num. Simu. **18(5)**, (2013) 1151-1161. (DOI:10.1016/J.CNSNS.2012.09.029)
10. Hastings S. P, Troy W. C. *Oscillating solutions of the Falkner-Skan equation for negative β*. SIAM J. Math Anal. **18(2)**, (1987) 422-429. (DOI:10.1137/0518032)
11. Yang H. T, Chien L. C. *Analytic solutions of the Falkner-Skan equation when β = -1 and γ = 0*. SIAM J. Appl. Math. **29(3)**, (1975) 558-569. (DOI:10.1137/0129047)
12. Riley N, Weidman P. D. *Multiple solutions of the Falkner-Skan equation for flow past a streching boundary*. SIAM J. App Math. **49(5)**,(1989)1350-1358. (DOI:10.1137/0149081)
13. Sachdev P. L, Kudenatti R. B, Bujurke N. M. *Exact analytic solution of boundary value problem for the Falkner-Skan equation*. Stud. Appl. Math. **120(1)**, (2008) 1-16. (DOI:10.1111/j.1467-9590.2007.00386.x)
14. Oskam B, Veldman A. E. P. *Branching of the Falkner-Skan solutions for $\lambda < 0$*. J. Engg. Math. **16(4)**, (1982) 295-308. (DOI:10.1007/BF00037732)
15. Liao S. J. *A unifromly valid analytic solution of two-dimensional viscous flow over a semi-infinite flate plate*. J. Fluid Mech. **385**, (1999) 101-128. (DOI:https://doi.org/10.1017/S0022112099004292)
16. Yang K. T. *Unsteady laminar BLs in an incompressible stagnation flow*. Trans. ASME: J. Appl. Mech. **25**, (1958) 421-427.
17. Philip M. a. K. H, Hui W. H. 1990 *Similarity solutions of the two-dimensional unsteady BL equations*. J. Fluid Mech. **216**, (1990) 537-559. (DOI:https://doi.org/10.1017/S0022112090000520)
18. Sattar M. A. *A local similarity transformation for the unsteady two-dimensional hydrodynamic BL equations of a flow past a wedge*. Int. J. App. Math. and Mech. **7(1)**, (2011)15-28.
19. Yuan S. W. *Foundation of Fluid mechanics*. Prentice-Hall International Inc., London, 1970.
20. Bender C. M, Orzag S. *Advanced mathematical methods for scientists and engineers*. McGraw-Hill, (1978).
21. Abramowitz M, Stegun I. *Handbook of mathematical functions with formulas, Graphs, and Mathematical Tables*. 9th edition. Dover, (1970).
22. Andrews L. C. *Special functions of mathematics for engineers*. 2nd edition. Oxford University Press, (1998).
23. Duck P. W, Dry S. L. *On a class of unsteady, non-parallel, three-dimensional disturbances to BL flows*. J. Fluid Mech. **441**, (2001) 31-65. (DOI:https://doi.org/10.1017/S0022112001004724)
24. Fang T. *Flow and mass transfer for an unsteady stagnation-point flow over a moving wall considering blowing effects*. J. Fluid Engg. **136(7)**, (2014) 071103-7. (doi:10.1115/1.4026665)
25. Kudenatti R. B, Shilpa P *Similarity solution of the unsteady boundary layer flow past a permeable wedge embedded in a porous medium*. j. Porous Media **22(6)**, (2019) 745-759. (DOI:10.1615/JPorMedia.2019029063)
26. Kudenatti R. B, Kirsur S. R, Achala L. N, Bujurke N. M. *Similarity Solution of the MHD boundary layer flow past a constant wedge within porous media*. Math. Probl. Eng., (2017) 1-11. (DOI:10.1155/2017/1428137)
27. Kudenatti R. B, ShashiProbha Gogate. *Modelling the fluid flow and mass transfer through porous media with Effective viscosity on the three- dimensional boundary layer*. j. Porous Media **22(11)**, (2018) 1069-1084. (DOI:10.1615/JPorMedia.2018021347)
28. Kudenatti R. B, Vanitha V. R. *Exact and Asymptotic solution of a steady two dimensional boundary layer of a Micropolar fluid flow past a moving wedge*. J. Phys.:Conf.Ser.1597012020, (2020).

Shilpa P.,
Department of Mathematics,
Dayananda Sagar Academy of Technology and Management,
Visvesvaraya Technological University, Belagavi
India.
E-mail address: shilpap80@gmail.com

and

Nagaraj C.,
Department of Mathematics,
Dayananda Sagar Academy of Technology and Management,
Visvesvaraya Technological University, Belagavi
India.
E-mail address: drnagarajc@gmail.com

and

Rakesh Kumar Singh.,
Department of Mathematics,
School of Engineering,
Dayananda Sagar University,
India.
E-mail address: rakeshsingh-maths@dsu.edu.in

and

Lakshmi B.,
Department of Mathematics,
K. S. School of Engineering and Management,
Visvesvaraya Technological University, Belagavi
India.
E-mail address: laksh94801@gmail.com

and

Vatsala G. A.,
Department of Mathematics,
Dayananda Sagar Academy of Technology and Management,
Visvesvaraya Technological University, Belagavi
India.
E-mail address: dr.vatsala.ga@gmail.com